

NANOPARTICLES

https://doi.org/10.1070/QEL16253

Effect of nanoparticle sizes on the extinction spectrum of colloidal solutions produced by laser ablation of gold in water

S.V. Starinskiy, Yu.G. Shukhov, A.V. Bulgakov

Abstract. **We have measured the extinction spectra of colloidal solutions of gold nanoparticles synthesised by nanosecond laser ablation in water for the conditions of a bimodal particle size distribution. The extinction spectra are analysed by using the Mie theory and the contribution of particles of different sizes to the radiation attenuation is established. A method is proposed for determining the concentrations of individual populations of particles in a solution on the basis of the spectral dependence of the extinction coefficient. Mechanisms of the nanoparticle formation during laser ablation of metals in liquids are discussed.**

Keywords: *laser ablation in liquids, colloidal solution, extinction spectrum, gold nanoparticles, bimodal particle size distribution, plasmon resonance, Mie theory.*

Nanoparticles of noble metals possess unique electronic, catalytic and optical properties, including localised surface plasmon resonance [1–3], which is of interest for many applications like solar energy, spectroscopy, sensor development and medicine. Optical properties of plasmon nanoparticles depend on their size, shape and concentration; therefore, it is important to have means for monitoring and controlling parameters of synthesised particles. One of the most effective and flexible methods for the synthesis of nanoparticles is laser ablation in liquids [4–8], which allows colloidal solutions to be produced with characteristics that cannot be achieved by other methods [8]. Thus, the method makes it possible to synthesise stable particles without foreign impurities and surfactants, which is important for many medical applications.

The most common method for analysing the sizes of colloidal nanoparticles is high-resolution electron microscopy [4–8], which, however, has a number of disadvantages in this case. The method does not allow one to analyse particles directly in a solution and to measure their concentration, whereas preparing samples for the analysis (deposition on a substrate) often leads to a change in the initial sizes of the particles. Other control methods, such as time-resolved X-ray scattering [9] or differential mobility analysis [10], are quite expensive and have a number of specific limitations. Amendola and Meneghetti [11] developed a method for estimating the average size of colloidal gold particles in the range from 4 to 25 nm on the basis of an analysis of their extinction spectrum by the Mie theory, which makes it possible to determine the concentration of particles in the solution and also to take into account their nonsphericity. However, the technique is not applicable in the case of a bimodal particle size distribution typical for colloids produced by laser ablation in liquids and often including populations of particles with very different sizes [4, 7, 8, 12–14].

In this paper, we study the extinction spectra of aqueous colloidal solutions for a bimodal distribution of nanoparticles synthesised by ablation of gold with nanosecond laser pulses. On the basis of the Mie theory, a method for calculating the spectra has been developed, which made it possible to estimate the contribution of different populations of nanoparticles to the attenuation of radiation and to determine their concentration in the solution.

A gold target (99.99% purity plate) was ablated by Nd:YAG laser pulses (wavelength, 1064 nm; pulse duration, 9 ns; and repetition rate, 5 Hz) along the normal to the surface. The sample was immersed in a cuvette with distilled deionised water (volume, 20 mL; height of a column of liquid above the target, 10 mm). Laser radiation was focused onto the surface in a spot with a diameter of ~1 mm with the help of a scanning optical system (folding prism and focusing lens), which allows the beam to move along the surface during the synthesis of the colloidal solution (the total number N of pulses varied in the range 3000–10000). In experiments, we used relatively low irradiation energy densities F_0 in the range 3–10 J cm^{-2}, slightly exceeding the gold ablation threshold in water (for our conditions ~2 J cm^{-2} [15]), when the formation of two populations of nanoparticles is clearly expressed. To investigate the optical properties of the obtained solutions, a DFS-458C diffraction spectrophotometer was applied. The size and shape of the nanoparticles were analysed using a JEOL-JEM2010 transmission electron microscope (TEM), samples for which were prepared by evaporation of several drops of a solution on a film of amorphous carbon deposited on a copper grid. The surface of the targets after irradiation was studied with a JEOL JSM-6700F scanning electron microscope (SEM).

Figure 1 shows a typical TEM image of the synthesised particles. Obviously, there are two populations, i.e. small nanoparticles with a characteristic size of ~10 nm, dominating in the solution, and a small number of large particles 50–200 nm in size. The shape of all the particles is close to spherical. The scatter of small particles in size is well approximated by the log-normal distribution

$$f(d) = \frac{A}{\sqrt{2\pi}\, wd} \exp\left[-\frac{\ln(d/d_a)}{2w^2}\right] \qquad (1)$$

S.V. Starinskiy, Yu.G. Shukhov, A.V. Bulgakov S.S. Kutateladze Institute of Thermophysics, Siberian Branch, Russian Academy of Sciences, prosp. Akad. Lavrent'eva 1, 630090 Novosibirsk, Russia; e-mail: bulgakov@itp.nsc.ru

Received 9 November 2016; revision received 6 February 2017
Kvantovaya Elektronika **47** (4) 343–346 (2017)
Translated by I.A. Ulitkin

with an average particle size d_a = 9 nm and a dispersion w = 0.4. Here A is a constant proportional to the total surface concentration of small particles. The distribution of large particles is difficult to estimate from the TEM images because of insufficient statistics, but we can assume that it is apparently quite wide (Fig. 1). The average size of small particles is virtually independent of the radiation energy density F_0 and the number N of pulses; the fraction of large particles decreases with increasing F_0 for the considered irradiation conditions near the ablation threshold.

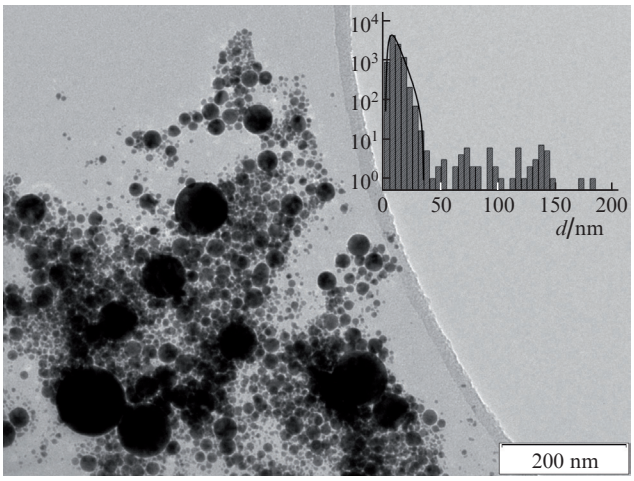

Figure 1. Typical TEM image of the particles produced by laser ablation of gold in water (laser energy density, F_0 = 8.4 J cm^{-2}; and the number of laser pulses, N = 10000). The inset shows a histogram of the particle size distribution constructed on the basis of an analysis of eight images for this ablation regime; the solid curve corresponds to distribution (1) for small particles.

Figure 2 shows the spectral dependences of the extinction coefficient $\gamma = \ln(I_0/I)$ for two regimes of solution synthesis, where I_0 and I are the intensities of incident radiation and radiation transmitted through the solution, respectively. At a wavelength of ~525 nm, the maximum attenuation of light is attained, which is typical for spherical gold particles in water [5, 7, 8]. The position of the peak of the plasmon resonance depends weakly on F_0, which confirms the data (obtained from TEM images) on the invariance of the distribution function of small particles, which make the main contribution to the attenuation of light. With decreasing F_0 the resonance peak becomes broader, and the extinction coefficient decreases in the long-wavelength region of the spectrum less sharply due to an increase in the fraction of large particles in the solution. These observations are also consistent with the results of the TEM analysis. Increasing the number of laser pulses leads to a linear increase in the amplitude of the extinction spectrum of the solution, indicating an increased concentration of the particles without changing their sizes.

To determine the contribution of particles of different sizes into the optical characteristics of colloidal solutions, we calculated the extinction spectra by using the full Mie theory [16], which provides for a spherical particle of radius R the expression for the extinction cross section σ_{ext}:

$$\sigma_{ext} = \frac{\lambda^2}{2\pi n_0^2} \sum_{i=1}^{\infty} (2i+1)\,\mathrm{Re}(a_i + b_i). \qquad (2)$$

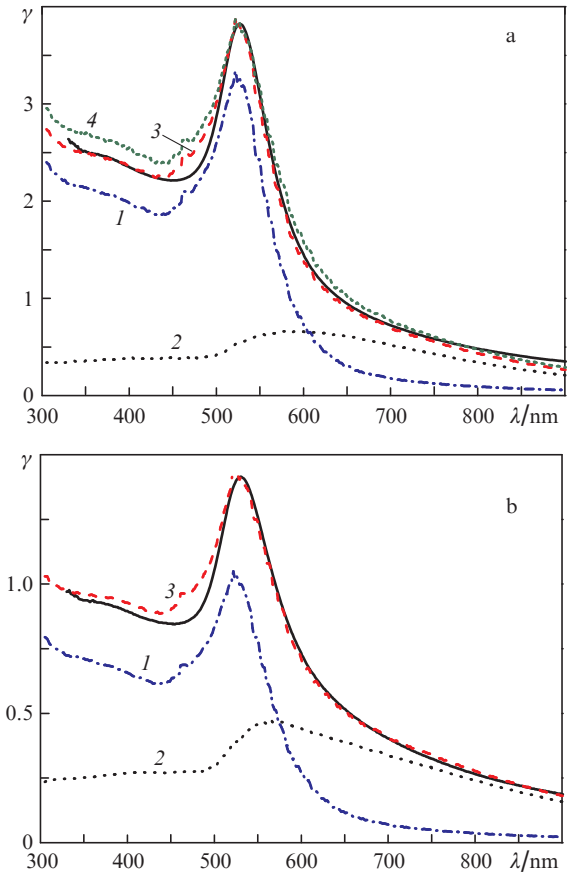

Figure 2. Experimental (solid curves) and calculated (*1–4*) extinction spectra of colloidal solutions of gold produced by laser ablation in water at F_0 = (a) 8.4 and (b) 5.5 J cm^{-2}. Curves (*1*) shows the contribution of small particles, curves (*2*) – the contribution of large particles, curves (*3*) – the total spectrum, curves (*4*) – the total spectrum for a fixed size of small particles (9 nm). Calculations were carried out for (a) n_s = 9.3×10^{12} cm^{-3}, n_l = 8×10^8 cm^{-3} and (b) n_s = 4.8×10^{12} cm^{-3}, n_l = 5.5×10^8 cm^{-3}.

Here λ is the laser wavelength; n_0 is the refractive index of the medium (for water, n_0 = 1.33 is assumed in the calculations); and $a_i(R)$ and $b_i(R)$ are the coefficients whose expressions have the form [16]

$$a_i = \frac{m\psi_i(mx)\psi_i'(x) - \psi_i'(mx)\psi_i(x)}{m\psi_i(mx)\eta_i'(x) - \psi_i'(mx)\eta_i(x)},$$

$$b_i = \frac{\psi_i(mx)\psi_i'(x) - m\psi_i'(mx)\psi_i(x)}{\psi_i(mx)\eta_i'(x) - m\psi_i'(mx)\eta_i(x)},$$

$$m = \frac{n_p(R)}{n_0},$$

$$x = \frac{2\pi n_0 R}{\lambda},$$

where n_p is the complex refractive index of the particle; and ψ_i and η_i are the spherical Riccati–Bessel functions. Calculation by formula (2) was limited to the second-order term describing the excitation of quadrupole electric field modes, which is acceptable for particles smaller than 200 nm [16]. Knowing the cross section $\sigma_{ext}(d)$, we can determine the measured

extinction coefficient γ for a solution containing particles of different sizes by using the relation

$$\gamma = L\sum_j v_j \sigma_{\mathrm{ext}\,j}, \qquad (3)$$

where v_j is the volume concentration of particles with a size d_j in the solution, and the summation is performed over all nanoparticle sizes; $\sigma_{\mathrm{ext}\,j} = \sigma_{\mathrm{ext}}(d_j)$; and $L = 10$ mm is the length of the optical path in the spectral measurements. It was assumed that the particle size distribution in the solution obeys the same log-normal distribution (1), so that $v_j = f(d_j)\Delta d$, where Δd is the size step in the summation in (3) (in calculations $\Delta d = 1$ nm for $d = 1-30$ nm and 10 nm for $d > 30$ nm). Consequently, if we confine ourselves to a contribution to the attenuation of radiation from only a population of small particles, the constant A in (1) is equal to the total volume concentration of these particles, n_s, whose value can be determined by comparing the absolute values of the extinction coefficients obtained in the calculations and in the experiment. The parameters d_a and w of distribution (1) were also varied in order to achieve a coincidence of the experimental and calculated spectra. In the calculations, the spectral dependences [17] were used for the optical characteristics of gold. In this case, the dependence of the permittivity of the particles on their size was taken into account [1].

The calculated extinction spectrum of the particles with an average size $d_{as} = 9$ nm and distribution (1) does not describe the experimental data in the long-wavelength region of the spectrum (see Fig. 2). The discrepancy was eliminated by taking into account the scattering and absorption of light by large particles. As a distribution of these particles in size, we also used the dependence (1) with free parameters d_{al}, w_l and $A = n_l$, which were found from the condition of the best agreement between the calculation results and the experiment (here the subscript 'l' refers to large particles, and n_l is the total volume concentration of these particles). In this case, the shape of the extinction spectrum is determined by the ratio of the concentrations n_s/n_l rather than by their absolute values. For the spectra in Fig. 2, we have found the following values: $d_{al} = 140$ nm (independent of F_0), $n_s/n_l = 1.2\times10^4$ (which agrees qualitatively with the TEM analysis in Fig. 1), $w_l = 0.2$ for $F_0 = 8.4$J cm^{-2} and $n_s/n_l = 9\times10^3$, $w_l = 0.5$ for $F_0 = 5.5$ J cm^{-2}. Note that for the correct description of the extinction spectrum, it is necessary to take into account the particle size distribution. Thus, the calculation for the case of small particles with a fixed size of 9 nm (with allowance for the contribution of large particles) does not describe the experimental spectrum in the short-wavelength region (Fig. 2a).

A comparison of the absolute values of the extinction coefficient obtained in the calculations and in the experiment made it possible to determine the concentrations of both populations of particles in the solution, which cannot be done on the basis of a TEM analysis. In particular, for $F_0 = 8.4$ J cm^{-2} and $N = 10000$ (Fig. 2a), the concentration of small particles ($d_{as} = 9$ nm) is $n_s = 9.3\times10^{12}$ cm^{-3}, and the concentration of large particles ($d_{al} = 140$ nm) is $n_l = 8\times10^8$ cm^{-3}, i.e., by four orders of magnitude lower. Knowing the concentrations, we can estimate the total masses of the particles in the solution, which were 1.8 mg for small particles and 0.6 mg for large particles. The total calculated mass of the particles (2.4 mg) is in good agreement with the result of direct weighing of the dry residue of the solution after evaporation of water (2.7 ± 0.1 mg).

It should be noted that the proposed method allows for some ambiguity in determining the sizes of colloidal nanoparticles from the extinction spectra. Thus, the spectra in Fig. 2 can be described equally well by varying the average size of small particles in the range of 6–12 nm at a slight correction of the size of large particles. Analysis of the spectra obtained under different conditions showed that the error in determining the sizes for small and large particles using the Mi theory is approximately ±30%.

The presence of two types of particles in the solution implies different mechanisms of their formation [4, 8, 14]. Presumably, small nanoparticles are formed due to nucleation and growth in a laser plasma [7, 14] or due to sputtering of a molten target under the action of vapour pressure [5, 13]; the main mechanisms for the formation of submicron particles are the emission of microdroplets in explosive ablation (phase explosion) [4, 12] and particle aggregation during the collapse of a cavitation bubble [8, 14]. Our experiments give information about the origin of large particles in the conditions under consideration. In particular, a phase explosion due to low-intensity laser pulses seems unlikely, since it manifests itself in a threshold manner at energy densities F_0 that are much higher than the ablation threshold [18, 19]. In the present study, large particles are observed near the ablation threshold, and their concentration decreases with increasing F_0. This behaviour is more typical for the emission of microdroplets from the molten surface due to its hydrodynamic instability, i.e., for a mechanism well known for nanosecond laser ablation in a vacuum or background gas [20–23]. Thus, experiments on the deposition of thin films during ablation of metals by low-intensity laser pulses demonstrate that emission from the surface of micron and submicron droplets decreases with increasing irradiation energy density [20, 24]. Analysis of laser spots by scanning electron microscopy shows that the initially polished surface of gold irradiated by 10 laser pulses in water acquires a small-scale wave-like structure (Fig. 3), evidencing the development of hydrodynamic instability of the melt [22, 25]. It counts in favour of this mechanism that large particles are spherical (Fig. 1), which is a less likely scenario in the aggregation of small particles [7],

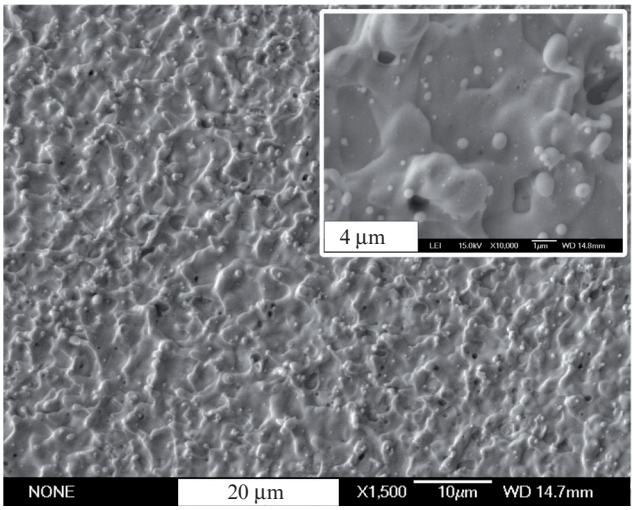

Figure 3. SEM image of the gold surface after irradiation ($F_0 = 8.4$ J cm^{-2}, $N = 10$). The inset shows a fragment of the surface on an enlarged scale.

although the coalescence of liquid nanoparticles in a cavitation bubble cannot be excluded. One can see from Fig. 3 that a fraction of the emitted particles is deposited on the surface of the target, which is apparently due to the reverse motion of the ablation products when the bubble collapses [14]. Irradiation with subsequent pulses can carry these particles back to solution as a result of shock cavitation.

Thus, based on the Mie theory, we have developed a method for analysing the extinction spectra of colloidal solutions containing populations of nanoparticles with widely differing masses, which allows one to determine the presence of bimodality in the particle size distribution from the spectral dependence of the extinction coefficient and also to estimate the average particle size and concentrations of particles of individual populations. The method has been tested for the case of gold nanoparticles in water, but it can also be used to analyse colloidal solutions of other metals synthesised by laser ablation in liquids.

Acknowledgements. The work was supported by the Russian Science Foundation (Grant No. 16-19-10506).

References

1. Kreibig U., Vollmer M. *Optical Properties of Metal Clusters* (Berlin-Heidelberg: Springer, 1995).
2. Link S., El-Sayed M.A. *J. Phys. Chem. B*, **103**, 8410 (1999).
3. Ghosh S.K., Pal T. *Chem. Rev.*, **107**, 4797 (2007).
4. Kabashin A.V., Meunier M. *J. Appl. Phys*., **94**, 7941 (2003).
5. Simakin A.V., Voronov V.V., Kirichenko N.A., Shafeev G.A. *Appl. Phys. A*, **79**, 1127 (2004).
6. Yang G.W. *Prog. Mater. Sci*., **52**, 648 (2007).
7. Amendola V., Meneghetti M. *Phys. Chem. Chem. Phys*., **11**, 3805 (2009).
8. Rehbock C., Jakobi J., Gamrad L., van der Meer S., Tiedemann D., Taylor U., Rath D., Barcikowski S., Belstein J. *Nanotechnol*., **5**, 1523 (2014).
9. Pleh A., Kotaidis V., Gresillon S., Dahmen C., von Plessen G. *Phys. Rev. B*, **70**, 195423 (2004).
10. Lenggoro I.W., Xia B., Okuyama K., de la Mora J.F. *Langmuir*, **18**, 4584 (2002).
11. Amendola V., Meneghetti M. *J. Phys. Chem. C*, **113**, 4277 (2009).
12. Nichols W.T., Sasaki T., Koshizaki N. *J. Appl. Phys*., **100**, 114912 (2006).
13. Kazakevich P.V., Simakin A.V., Voronov V.V., Shafeev G.A. *Appl. Surf. Sci*., **252**, 4373 (2006).
14. Wagener P., Ibrahimkutty S., Menzel A., Plech A., Barcikowski S. *Phys. Chem. Chem. Phys*., **15**, 3068 (2013).
15. Starinskiy S.V., Shukhov Yu.G., Bulgakov A.V. *Appl. Surf. Sci.*, **396**, 1765 (2017).
16. Bohren C.F., Huffman D.R. *Absorption and Scattering of Light by Small Particles* (New York: John Wiley & Sons, 1983).
17. Johnson P.B., Christy R.W. *Phys. Rev. B*, **6**, 4370 (1972).
18. Bulgakova N.M., Bulgakov A.V. *Appl. Phys. A*, **73**, 199 (2001).
19. Bulgakova N.M., Evtushenko A.B., Shukhov Yu.G., Kudryashov S.I., Bulgakov A.V. *Appl. Surf. Sci.*, **257**, 10876 (2011).
20. Van de Riet E., Nillesen C.J.C.M., Dieleman J. *J. Appl. Phys*., **74**, 2008 (1993).
21. Brailovsky A.B., Gaponov S.V., Luchin V.I. *Appl. Phys. A*, **61**, 81 (1995).
22. Bennett T.D., Grigoropoulos C.P., Krajnovich D.J. *J. Appl. Phys*., **77**, 849 (1995).
23. Starinskiy S.V., Shukhov Yu.G., Bulgakov A.V. *Tech. Phys. Lett*., **42** (4), 411 (2016) [*Pis'ma Zh. Tekh. Fiz*., **42** (8), 45 (2016)].
24. Siew W.-O., Lee W.-K., Wong H.-Y., Yong T.-K., Yap S.-S., Tou T.-Y. *Appl. Phys. A*, **101**, 627 (2010).
25. Stratakis E., Zorba V., Barberoglou M., Fotakis C., Shafeev G.A. *Appl. Surf. Sci.*, **255**, 5346 (2009).